



Palaeoenvironmental turnover across the Ypresian–Lutetian transition at the Agost section, Southeastern Spain: In search of a marker event to define the Stratotype for the base of the Lutetian Stage

Silvia Ortiz^{a,b,*}, Concepción Gonzalvo^a, Eustoquio Molina^a, Francisco J. Rodríguez-Tovar^c, Alfred Uchman^d, Noël Vandenberghe^e, Edwin Zeelmaekers^e

^a Departamento de Ciencias de la Tierra, Universidad de Zaragoza, E-50009 Zaragoza, Spain

^b Department of Earth Sciences, University College London, WC1E 6BT London, United Kingdom

^c Departamento de Estratigrafía y Paleontología, Universidad de Granada, E-18071 Granada, Spain

^d Institute of Geological Sciences, Jagiellonian University, PL-30063 Krakow, Poland

^e Departement Geologie, University of Leuven, B-3000 Leuven, Belgium

ARTICLE INFO

Article history:

Received 16 April 2008

Received in revised form 26 August 2008

Accepted 3 September 2008

Keywords:

Lutetian GSSP

Foraminifera

Trace fossils

Mineralogy

Palaeoenvironment

Agost

Southeastern Spain

ABSTRACT

Marker events to define the stratotype for the base of the Lutetian Stage are poorly defined. To elucidate such markers and characterize palaeoenvironmental turnovers, we conducted an integrated study of the Ypresian–Lutetian (Y–L; early-middle Eocene) transition at the continuous Agost section (southeastern Spain). This 115-m-thick section, which consists of hemipelagic marls intercalated with hemipelagic limestones and turbidity sandstones, spans from planktic foraminiferal Zones P9 to P12 (E7 to E10) and calcareous nannofossil Zones CP11 to CP14a (NP13 to NP16). We report quantitative analyses of planktic and benthic foraminifera and characterization of trace fossil assemblages that are integrated with mineralogical analyses. Relative to benthic forms, planktic foraminifera constitute more than 80% of the foraminiferal assemblage. We found that the most abundant planktic species belong to the genera *Acarinina*, *Morozovella*, *Subbotina*, and *Pseudohastigerina*. Benthic foraminiferal assemblages are strongly dominated by calcareous taxa, with bolivinids being the most abundant group. Trace fossils showed the succession *Nereites*–*Zoophycos*–*Cruziana* ichnofacies throughout the Agost section. In addition to changes in palaeobathymetry, we deduced that quantity and quality of organic matter flux influenced by turbidity currents are the main factors controlling benthic assemblages. We distinguished several mineralogical boundaries at the Agost section, each associated with lithological facies changes suggesting a change in provenance rather than changes in weathering conditions. We made three observations that indicate an increase in sea water temperatures or a possible hyperthermal event related to the first occurrence (FO) of hantkeninids (i.e., the P9/P10 boundary): 1) a distinct peak in abundance of the benthic foraminifera *Aragonia aragonensis*; 2) the low-diversity of benthic foraminiferal assemblages; and 3) the occurrence of the planktic foraminifera *Clavigerinella eocenica* and *Clavigerinella jarvisi*. Benthic foraminiferal and trace fossil assemblages also suggest an associated relative fall of sea level from upper-middle bathyal to sublittoral depths. These characteristic indicators point to this boundary as a promising feature for defining the Global Stratotype Section and Point (GSSP) for the base of the Lutetian Stage. However, complementary magnetobiostratigraphic studies carried out at the Agost section point to the FO of calcareous nannofossil *Blackites inflatus* (base of CP12b), which occurred 3–5 Myr before the P9/P10 boundary, as the most suitable

* Corresponding author. Department of Earth Sciences, University College London, WC1E 6BT London, United Kingdom. Tel.: +34 976 761000x3160; fax: +34 976 761106.

E-mail addresses: silortiz@unizar.es (S. Ortiz), concha@unizar.es (C. Gonzalvo), emolina@unizar.es (E. Molina), fjrtovar@ugr.es (F.J. Rodríguez-Tovar), Alfred.uchman@uj.edu.pl (A. Uchman), Noel.Vandenberghe@geo.kuleuven.be (N. Vandenberghe), Edwin.Zeelmaekers@geo.kuleuven.be (E. Zeelmaekers).

primary marker event. Whatever the marker event chosen, all the successive events recognized at the Agost section allow a complete characterization of the Y–L transition, and thus this section may be a suitable candidate to locate the GSSP for the Ypresian/Lutetian boundary.

© 2008 Elsevier B.V. All rights reserved.

1. Introduction

The Ypresian–Lutetian (Y–L) or early-middle Eocene transition has received comparatively little attention, traditionally overshadowed by events related to the Palaeogene Epochs boundaries. However, in search of sections to define the Global Stratotype Section and Point (GSSP) for the base of the Lutetian Stage, i.e., the Ypresian/Lutetian (Y/L) boundary, an International Working Group of the International Sub-commission on Palaeogene Stratigraphy (ISPS) is advancing towards establishment of a chronostratigraphic frame for the Y–L transition (e.g., Molina et al., 2000, 2006; Bernaola et al., 2006; Payros et al., 2007; Larrasoña et al., in press). This coordinated study effort shows that events traditionally used to identify the Y/L boundary occur at different levels. Examples include first occurrence (FO) of the planktic foraminifera *Hantkenina nuttalli* or base of Zone P10 (Berggren et al., 1995); FO of the planktic foraminifera *Guembeltrioides nuttalli* or base of Zone E8 (Berggren and Pearson, 2005, 2006); FO of the calcareous nannofossil *Blackites inflatus* or base of Zone CP12b (Okada and Bukry, 1980); and the boundary between shallow benthic foraminiferal Zones SBZ12 and SBZ13 (Serra-Kiel et al., 1998). The FO of *H. nuttalli*, a junior synonym of *Hantkenina mexicana* (Pearson et al., 2006), is widely accepted as the main event identifying the Y/L boundary, which has traditionally been correlated with the top of Chron C22n (Lowrie et al., 1982; Napoleone et al., 1983).

The early Eocene was the warmest period of the Cenozoic (Early Eocene Climatic Optimum–EECO) (e.g., Zachos et al., 2001). The global warming peaked with an extreme, short-term global warming event, the Palaeocene–Eocene Thermal Maximum (PETM). This time period was characterized by negative oxygen and carbon isotope excursions and distinct shifts in biota such as the 30–50% extinction of deep-sea benthic foraminiferal species (e.g., Thomas, 2003). There have been identified several events similar to the PETM but of lesser intensity (called hyperthermals) through late Palaeocene to early Eocene, associated with dissolution horizons, isotope anomalies and benthic foraminiferal assemblage changes, e.g., Elmo and X events, dated at ~53.5 and ~52 Ma, respectively (e.g., Lourens et al., 2005; Kroon et al., 2007) with the latest of these events related to the Y/L boundary (Thomas and Zachos, 2000). At the Fortuna section (Betic Cordillera, southeastern Spain), located close to the Agost section, a possible hyperthermal event was proposed related to the Y/L boundary (Ortiz and Thomas, 2006). Global warming was followed by a long stepped cooling trend through the middle and late Eocene (49–34 Ma) with much of the change occurring over the early middle Eocene (50 to 48 Ma) (Zachos et al., 2001), i.e., the Y–L transition.

Following Remane et al. (1996), a boundary stratotype should be defined in a suitable marine continuous section. Because the base of the Lutetian stage defined in the Paris

Basin corresponds to a hiatus (Lapparent, 1883; Blondeau, 1981), the marine continuous section should occur outside of this basin. The Agost section is continuous (Larrasoña et al., in press), offering the possibility of evaluating palaeobathymetric turnover as an additional marker event for the Y/L boundary. Moreover, the boundary level must be chosen within a series of successive events in order to enable a reliable approximation in the absence of the primary marker. The Agost section includes all the events that might be selected as marker events for the Y/L boundary.

Larrasoña et al. (in press) provide an integrated magnetostratigraphic calibration based on foraminifera and calcareous nannofossils for the Agost section. Their results largely conform to the calibration proposed in the Gorron-datxe section of northern Spain (Bernaola et al., 2006; Payros et al., 2007) and further suggest a revision is in order for the standard calibration schemes for the Y–L transition (Berggren et al., 1995; Luterbacher et al., 2004; Berggren and Pearson, 2005, 2006; Pearson et al., 2006). In particular, the Zones P10 and E8 are found within Chron C20r, at a much younger age between 3 and 5 Myr. Payros et al. (2007) and Larrasoña et al. (in press) argue that a possible delay in the appearance of the species that define Zones P10 and E8, *Hantkenina mexicana* and *Guembeltrioides nuttalli* respectively, could be due to environmental factors because these taxa are usually rare outside the tropical belt. On the contrary, the FO of *Blackites inflatus* (base of CP12b) is found within Chron C21r, which matches the magnetostratigraphically calibrated age of ca. 48 Ma (middle part of C21r) considered in standard calibration schemes. This paper is part of that integrated study of the Agost section with the goal of identifying the base of the Lutetian Stage. We provide a quantitative analysis of benthic and planktic foraminiferal assemblages, characterize trace fossil assemblages, and mineralogical analyses in order to infer palaeoenvironmental and palaeobathymetric turnovers across the Y–L transition. This time interval marks an important step in Cenozoic climate evolution and thus further study will help identify a marker event for the base of the Lutetian Stage or, alternatively, elucidate other events at the chronostratigraphic boundary.

2. Material and methods

The Agost section is located in the Betic Cordillera of southeastern Spain, about 100 km to the east of the Caravaca section, a well-known Palaeogene section. The Agost section lies about 83 km to the northeast of the Fortuna section, which also spans the Y–L transition (Fig. 1). The outcrop we studied is about 1 km north of the Agost village (Alicante region), in the Lomas de la Beata area. This section is located close to the section studied previously by Molina et al. (2000), but offers better outcrop and fossil preservation conditions (Larrasoña et al., in press).

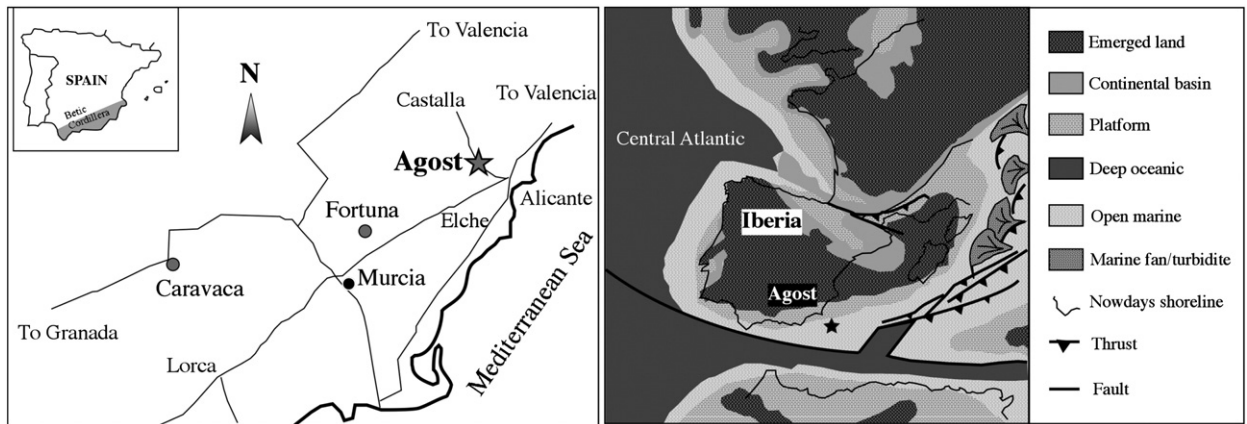


Fig. 1. Location of the Agost section and palaeogeographical reconstruction of the Iberian Peninsula at the Ypresian–Lutetian transition. Modified from Martín-Algarra and Vera (2004).

The Agost section is composed of 115 m of marls with intercalated limestone and sandstone beds. The marls and limestones correspond to hemipelagic sediments and predominate in the lower and upper parts of the section. The middle upper part of the section is mainly composed of sandstones that correspond to slope deposits. During the Eocene, the study area belonged to the passive margin of Iberia where carbonate sedimentation in the platform with abundant macroforaminifera gave way to pelagic sediments, turbidites, and mass flow deposits in the continental slope located to the south (Alonso-Zarza et al., 2002) (Fig. 1).

For biostratigraphic control we follow Larrasoña et al. (in press) who identified the Zones P9 to P12 (E7 to E10) of planktic foraminifera, Zones CP11 to CP14a (NP13 to NP16) of calcareous nannofossils, and Zones SBZ11 to SBZ15 of large benthic foraminifera. They also provide a magnetobiostratigraphic calibration, identifying Chrons C22n to C19r. In this paper, planktic foraminiferal taxa are updated following Berggren and Pearson (2006) (Appendix A).

For the study of planktic and small benthic foraminifera, we collected 86 samples throughout the section, most of them in marls, with closer-spaced sampling around meter 83.6, at the P9–P10 Zones transition (Figs. 2–4). We first disaggregated samples in water with diluted H_2O_2 and we washed them through a 100 μm sieve. We then cleaned each sample using ultrasonic agitation and repeated washes and sieving until a clean foraminiferal residue was obtained. The residue was then dried at 50 °C. We based quantitative and taxonomic analyses of planktic and benthic foraminifera (Appendices A and B) on representative random splits of more than 300 specimens (using a modified Otto micro-splitter) from each of 57 samples for planktic foraminifera, and from each of 21 samples for benthic foraminifera. We searched the remaining residue for rare species, particularly opportunistic species such as *Aragonia aragonensis*. We mounted representative specimens on microslides for identification and permanent record at the Departamento de Ciencias de la Tierra at the Universidad de Zaragoza, Spain. Scanning electron microscope images of selected planktic and benthic foraminifera from the Agost section can be seen in Larrasoña et al. (in press).

We classified benthic foraminifera at the generic level following Loeblich and Tappan (1988), and when possible, benthic foraminifera were identified at the specific level. We largely follow the taxonomy of Ortiz and Thomas (2006) and references therein. The most common and significant species with the original reference are listed in Appendix A.

We have used the morphotype analysis of benthic foraminifera (e.g., Corliss, 1985; Jones and Charnock, 1985; Corliss and Chen, 1988) to infer probable microhabitat preferences and environmental parameters such as the nutrient supply to the seafloor and seawater oxygenation (e.g., Bernhard, 1986; Jorissen et al., 1995). However, these data must be interpreted with caution since microhabitat assignments on the basis of morphology have only a 75% accuracy (Buzas et al., 1993). In Appendix B.2 we assign each taxon to one morphogroup and its more probable inferred microhabitat.

We performed ichnological research through the succession based on detailed outcrop observations. These observations include trace-fossil features and quantitative data, together with laboratory ichnofabric analysis. We collected specimens of trace fossils and samples for ichnofabric analyses from selected beds and observed in variable oriented, polished surfaces (Fig. 5, Plate I). We oiled surfaces in order to improve color contrast and to facilitate the analysis of ichnological details such as filling material and burrow boundary.

Our analysis of the (clay) mineralogy is based on quantitative bulk analysis and clay extraction for qualitative analyses, each of which depend on X-ray diffraction (XRD) measurements. We analyzed bulk mineralogy following the method of Środoń et al. (2001) and we used the QUANTA software for the subsequent data-analysis (Chevron proprietary software; Mystkowski et al., 2002). This is currently the most accurate way to determine the overall quantitative composition of clay-bearing sediments (Omotoso et al., 2006). This method allows for the determination of the quantitative composition of a sample for all non-clays and the clay minerals assembled in several groups. In this study we assembled clay minerals into 3 groups: “kaolinite”, “2:1 dioctahedral clays and micas” (= illite/smectite/illite-smectite/micas) and

“palygorskite”. The reported results (Fig. 6, Appendix B.3) were normalized to 100 wt.%, with a large majority of the unnormalized totals ranging between 96–103 wt.%.

To obtain more detailed information about the clay minerals, we extracted them from bulk sediment. We thus removed all cementing agents (carbonates, organic matter and Fe-oxides) following the procedures of Jackson (1975). After these treatments we separated the fractions <0.2 µm and <2 µm by centrifugation and made, respectively, oriented sedimentation slides and smears of these fractions. We then registered them using XRD in different states (air-dry, ethylene glycol saturated, heated to 550 °C/1 h) to permit standard clay identification techniques (e.g., Moore and Reynolds, 1997). This allowed detection of traces of chlorite, undetectable in the bulk analysis. Moreover, we also determined if the main component of the bulk quantified “2:1 dioctahedral clays and micas” group consists primarily of illite (I) or mixed-layered illite-smectite (IS) and smectite (S), or rather equal quantities of both. We applied the technique of Środoń (1981) on the XRD patterns to determine the exact percentage of S layers in the IS, providing an extra tool for qualitative characterization of the clay mineral content.

3. Results

3.1. Planktic foraminifera

Although planktic foraminiferal tests were filled in with sediment and recrystallized, we found that assemblages were nevertheless well preserved. Planktic assemblages composed more than 80% of total foraminifera. The most abundant species belonged to the genera *Acarinina*, *Morozovella*, *Subbotina*, and *Pseudohastigerina* (Appendix B.1). Other genera were less frequent but we found some to be very distinctive and stratigraphically significant; *Hantkenina*, *Clavigerinella*, and *Globigerinatheka* are important examples (Fig. 2).

From base to top of the section we identified the following biozones: P9, P10, P11, and P12 of the Berggren et al. (1995) biozonation; E7, E8, E9, and E10 of the Berggren and Pearson (2005) biozonation; and *Acarinina pentacamerata*, *Turborotalia frontosa*, *Acarinina praetopilensis*, *Hantkenina mexicana*, and *Globigerinatheka subconglobata* of the Gonzalvo and Molina (1998) biozonation. The index species *Astrorotalia* (= *Planorotalites*) *palmerae* of Zone P9 is absent in the Agost assemblages, but this zone can be recognized by the presence of *A. pentacamerata*, *Acarinina bullbroki*, *Acarinina soldadoensis*, *Subbotina inaequispira*, *Turborotalia frontosa*, *Morozovella caucasica*, and *Morozovella aragonensis*.

The FO of *Guembeltrioides nuttalli* in our samples occurs prior to the FO of *Hantkenina mexicana*, which is the index of Zone P10. According to Berggren and Pearson (2005), *G. nuttalli* characterizes the base of Zone E8, which would be equivalent to Zone P10 of Berggren et al. (1995). The non-simultaneous appearance of these two species indicates that this interval is

very expanded and continuous. Furthermore, the occurrence of *Hantkenina* cf. *singanae* at meter 83.6 of the section and its gradual evolutionary transition to *H. mexicana* indicates that the FO of *H. mexicana* at the Agost section is quite isochronic.

The most significant turnover in planktic foraminifera in our study occurs around meter 80. *Clavigerinella eocaenica* and *Clavigerinella jarvisi* occur just before the appearance of *Acarinina rohri*, *Acarinina topilensis*, and *Hantkenina mexicana*. This excursion of tropical species might be the result of an increase of seawater temperature.

3.2. Benthic foraminifera

We observed benthic foraminiferal assemblages dominated by calcareous taxa (95–99% of the assemblages) that totaled approximately 50 genera. However, benthic foraminifera in our samples were highly dominated by groups such as bolivinids, *Cibicides* spp., asterigerinids, and *Angulogerina* spp. Other common groups included *Anomalinoidea* spp., buliminids, and *Cibicidoides* spp. (Fig. 3). The most common calcareous species that we found were *Bolivinoidea crenulata*, *Angulogerina muralis*, *Lobatula lobatula*, *Bulimina alazanensis*, *Cibicidoides acutus*, *Cibicidoides eocaenus*, and *Hanzawaia amophila* (Fig. 4). The scarce and low-diversity agglutinated foraminiferal assemblages are dominated by cylindrical tapered genera such as *Clavulinoides*, *Gaudryina*, *Vulvulina*, and *Spiroplectinella*, with *Clavulinoides angularis* being the most abundant agglutinated species.

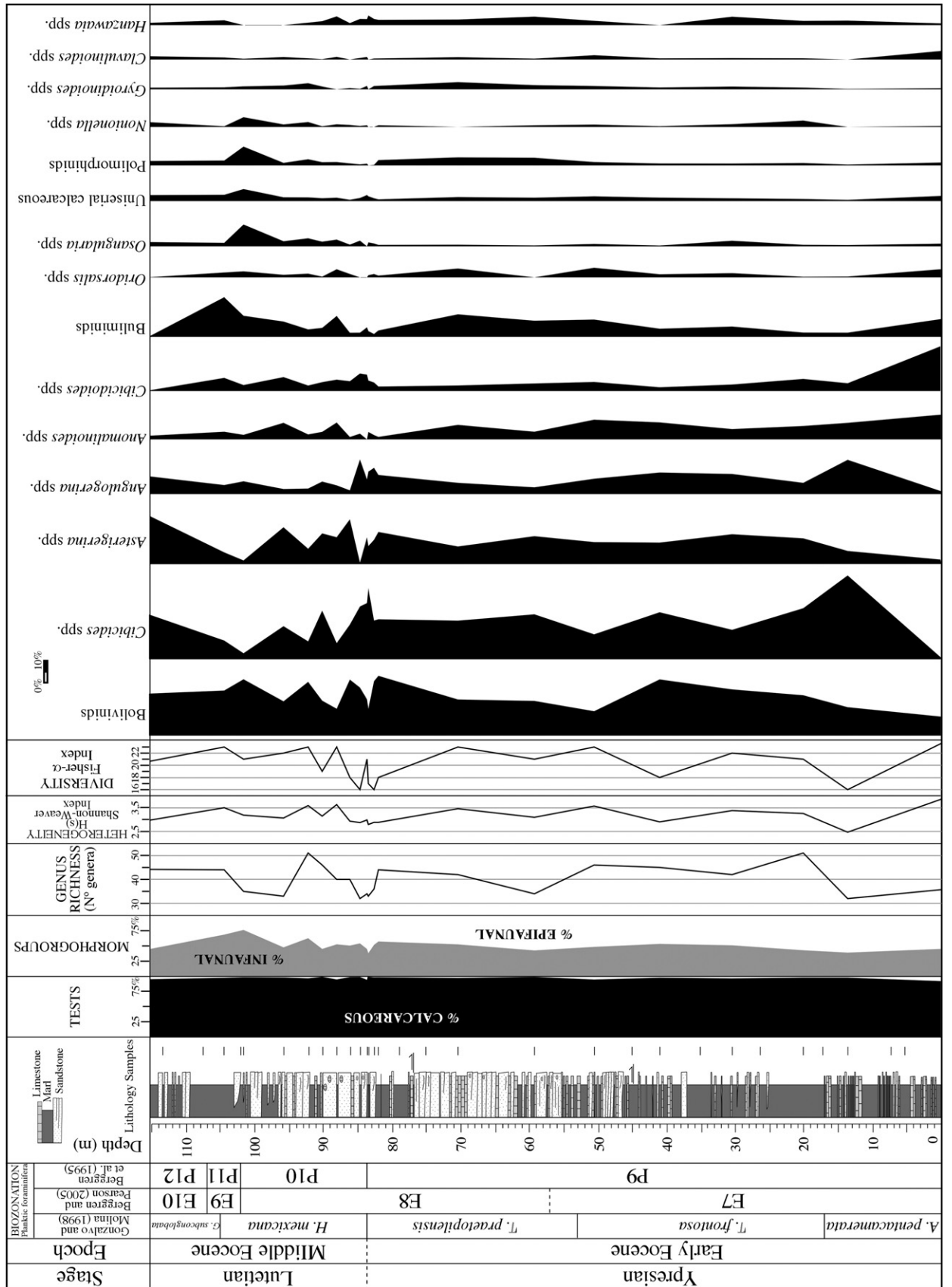
Benthic foraminiferal assemblages consisted of about equal abundance of epifaunal and infaunal morphogroups (Fig. 3, Appendix B.2). However, we observed an increase of infaunal morphogroups abundance towards the top of the section. Planoconvex/flattened trochospiral taxa such as *Cibicides* spp. and *Cibicidoides* spp. dominate the epifaunal morphogroups, whereas flattened and cylindrical taxa such as bolivinids, buliminids, and *Clavulinoides* spp. dominate the infaunal morphogroups.

Benthic foraminiferal assemblages contained peaks in relative abundance of several taxa. *Bulimina trinitatis* showed a peak in abundance at meter 50.5 (*Turborotalia frontosa* Zone). At the P9/P10 boundary, *Gaudryina* sp. showed a small peak in abundance. *Aragonia aragonensis* has a peak in abundance at meter 86, a few meters above the FO of *Hantkenina mexicana* (P9/P10 boundary). *Buliminella grata*, *Buliminella beaumonti*, and *Turrilina brevispira* showed a peak in abundance at meter 104.5 (*H. mexicana* Zone).

Diversity indices reach minimum values close to the CP12a/b boundary, at the lower part of the section (meter 13.2), and close to the P9/P10 boundary (Fig. 3). The appearances are not common, but their number is higher than the number of disappearances at specific level. The most characteristic FO that we observed is that of *Bulimina* aff. *midwayensis* at meter 88 (*Hantkenina mexicana* Zone).

We did not observe significant changes in heterogeneity throughout the section, a result due to the high dominance of

Fig. 2. Occurrence and relative abundances of the most characteristic planktic foraminiferal species across the Ypresian–Lutetian transition at the Agost section. A. *Acarinina*; C. *Clavigerinella*; G. *Guembeltrioides*; Gb. *Globigerinoides*; Gl. *Globigerinatheka*; H. *Hantkenina*; I. *Igorina*; M. *Morozovella*; Mo. *Morozovelloides*; P. *Pseudoglobigerinella*; Pr. *Parasubbotina*; Ps. *Pseudohastigerina*; S. *Subbotina*; T. *Turborotalia*.



several groups. Bolivinids are infaunal taxa correlated to high organic carbon flux rates at the seafloor. This group's strong dominance within other studies has generally been correlated with low oxygen conditions (e.g., Murray, 1991, 2006; Gooday, 1994; Bernhard and Sen Gupta, 1999; Thomas et al., 2000). However, bolivinids and other deep infaunal taxa have been recorded in environments with well-oxygenated bottom waters (e.g., Fontanier et al., 2005; Jorissen et al., 2007). Moreover, epifaunal taxa never comprise more than 40% of the assemblage except at the top of P10 and E9 Zones at the upper part of the Agost section. Asterigerinids are another dominant group that mainly occurs epiphytically in shallow water (e.g., Murray, 1991, 2006). We consider asterigerinids to be allochthonous, having been transported downslope due to the turbidity currents or by floating plant material. The high abundance of *Cibicides* spp. in our samples could also be a consequence of the turbidity currents and then, considered allochthonous, but they are usually found attached at hard substrates in high-energy settings (e.g., Murray, 1991, 2006). Intensified bottom-water currents (e.g., slope currents) have been shown to influence the microhabitat and composition of the benthic foraminiferal fauna (e.g., Lutze and Altenbach, 1988; Mackensen et al., 1995; Schönfeld, 1997, 2002a,b). *Lobatula lobatula* (*Cibicides lobatulus*) is a typical epifaunal species which seems to be closely linked to near-bottom currents for its nutritional needs (Altenbach et al., 1999). This species is a main component of the *Angulogerina angulosa* assemblage correlated to sandy sediments and strong and persistent near-bottom currents in the South Atlantic Ocean (Mackensen et al., 1995). *Angulogerina angulosa* is not abundant at the Agost section. However, *Angulogerina muralis* is abundant at the Agost section and could probably be considered an analogue of *A. angulosa* since we have commonly observed it in other Eocene turbiditic section in the Betic Cordillera of southeastern Spain (e.g., Molina et al., 2006; Ortiz and Thomas, 2006).

3.3. Trace fossils

In our samples the Y–L transition interval at the Agost section revealed a moderately abundant and moderately diverse trace fossil assemblage. It includes ichnogenera *Arenicolites*, *Chondrites*, *Diplocraterion*, *Helminthorhapha*, *Ophiomorpha*, *Paleodictyon*, *Planolites*, *Scolicia*, *Skolithos*, *Thalassinoides*, *Trichichnus*, and *Zoophycos* (Fig. 5, Plate I). Vertical distribution and relative abundance of these trace fossils showed a significant stratigraphic differentiation. Apart from the more or less continuous record of *Planolites* throughout our samples, we distinguished four stratigraphic intervals (A–D) on the basis of composition and abundance of trace fossils (Fig. 5). The lowest interval A (*Acarinina pentacamerata* Zone) was characterized by the presence of *Paleodictyon*, *Ophiomorpha*, and the punctual record of *Scolicia*, together with a high abundance of *Zoophycos*. The higher interval B (*A. pentacamerata* and *Turborotalia frontosa* Zones) was differentiated by the continuous distribution of *Zoophycos* (only punctual records in the interval C). The intermediate interval C (*T. frontosa* and *Acarinina praetopilensis* Zones) was characterized by the

continuous distribution of *Thalassinoides*, as well as by the occurrence of *Diplocraterion* in the lower part of the interval and the continuous presence of *Arenicolites* in the upper part. The topmost interval D (*Hantkenina mexicana* and *Globigerinatheka subconglobata* Zones) is defined by the comparative scarcity of biogenic structures, showing the impoverishment of trace fossil (e.g., *Chondrites*, *Planolites*, *Thalassinoides*), most of them only with punctual records.

Presence of *Paleodictyon*, *Ophiomorpha* (*O. annulata*, *O. rudis*), *Scolicia*, and *Zoophycos* in the lowermost of our A interval could be indicative of the *Nereites* ichnofacies. Particularly significant is the occurrence of graphoglyptids that are typical of the *Nereites* ichnofacies. The remaining ichnotaxa are also components of the *Zoophycos* and even *Cruziana* ichnofacies, including *Chondrites*, *Planolites*, and *Thalassinoides*. Upward, the disappearance of *Paleodictyon* together with the predominant record of *Zoophycos* (interval B) could be indicative of the progressive change towards the *Zoophycos* ichnofacies. Up the section (intervals C and D), *Zoophycos* almost disappears and is replaced gradually by the continuously occurring *Thalassinoides*, *Diplocraterion*, and *Arenicolites*. These three ichnotaxa are elements of the *Cruziana* ichnofacies, as well as *Chondrites* and *Planolites*. The punctual records of *Zoophycos* and *Skolithos* can be also included in the context of this ichnofacies. Thus, from bottom (interval A) to top of the succession (interval D) we observed a gradation of *Nereites*–*Zoophycos*–*Cruziana* ichnofacies.

Trace fossil assemblages in flysch deposits show marked inter- and intrabasinal variations (e.g., Uchman et al., 2004). The *Nereites* ichnofacies has been well characterized in Eocene flysch deposits (e.g., Tunis and Uchman, 1992, 1998; Uchman 2001; Uchman et al., 2004, and references therein) where it shows a great diversity of trace fossils and a variability related to palaeoenvironmental evolutionary and taphonomic changes. In most cases, sub-ichnofacies *Nereites*, *Paleodictyon*, and *Ophiomorpha rudis* can be distinguished within the *Nereites* ichnofacies (Uchman, 2001; Tunis and Uchman, 2003; Uchman et al., 2004). The ichno-assemblage we observed from interval A fits the *Ophiomorpha rudis* ichnosubfacies which is typical of sandy-rich proximal parts of turbiditic systems (Uchman, 2001, 2006).

Diplocraterion is typical of the *Skolithos* ichnofacies, but can occur in the *Cruziana* ichnofacies, especially in its proximal variant, in storm beds (e.g., Pemberton et al., 2001). Its occurrence in interval C, together with *Arenicolites* and *Skolithos*, can be related to post-storm opportunistic colonization of sandstone beds. Co-occurrence of horizontal trace fossils (*Thalassinoides*, *Planolites*) can be related to inter-storm sedimentation.

3.4. Mineralogy

Based on the results of the quantitative and qualitative mineralogical analyses, we distinguished four mineralogical boundaries in the studied section (Fig. 6; Appendix B.3). We observed a first mineralogical boundary located between meter 40 and 45, above which the clay mineralogy is clearly

Fig. 3. Occurrence and relative abundances of the most characteristics benthic foraminiferal groups and characteristics of benthic foraminiferal assemblages across the Ypresian–Lutetian transition at the Agost section. Relative percentages of calcareous and agglutinated tests, relative percentages of infaunal and epifaunal morphogroups, genus richness, Shannon–Weaver heterogeneity and Fisher- α Index.

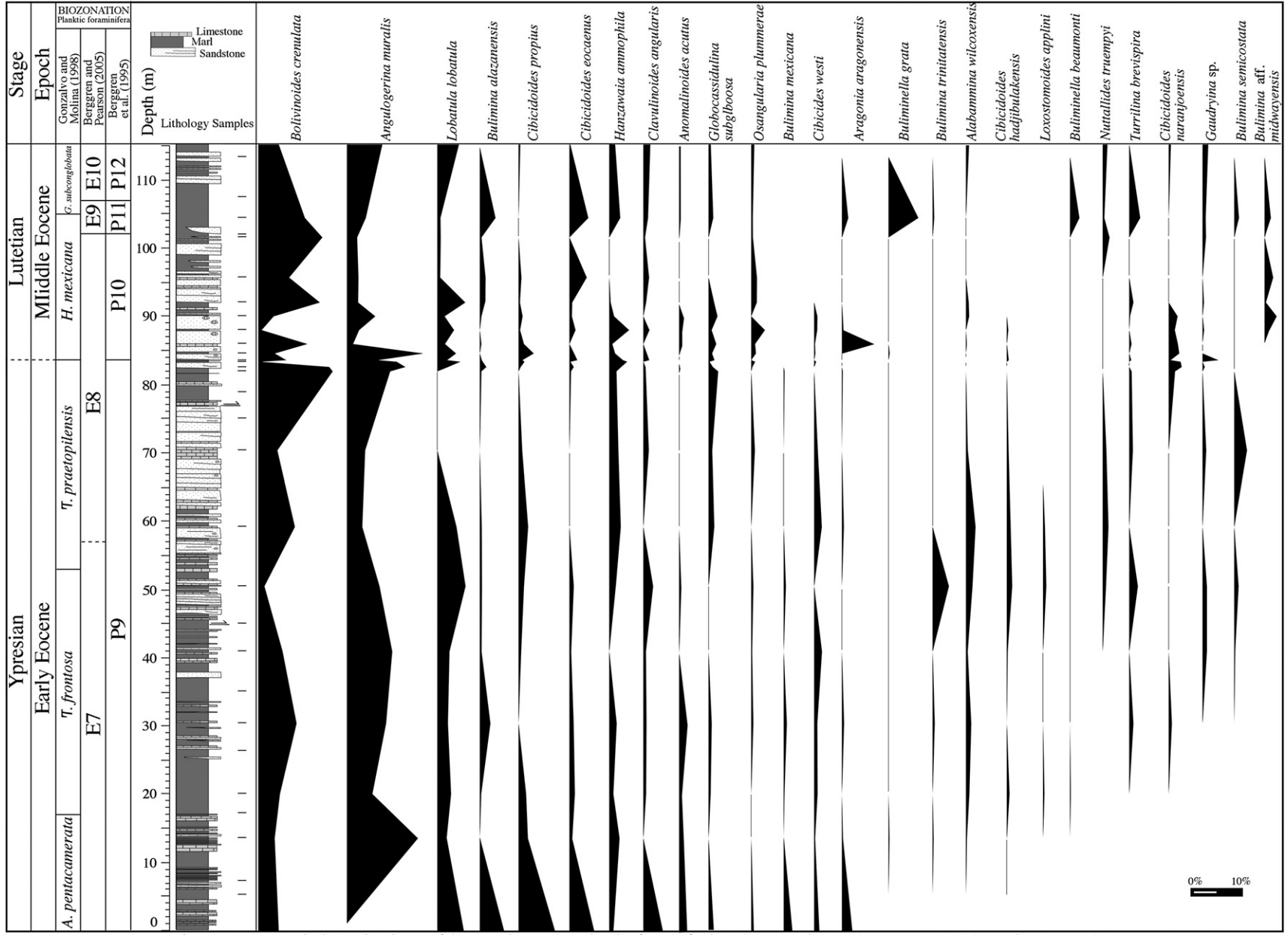


Fig. 4. Occurrence and relative abundances of the most characteristic benthic foraminiferal species across the Ypresian-Lutetian transition at the Agost section.

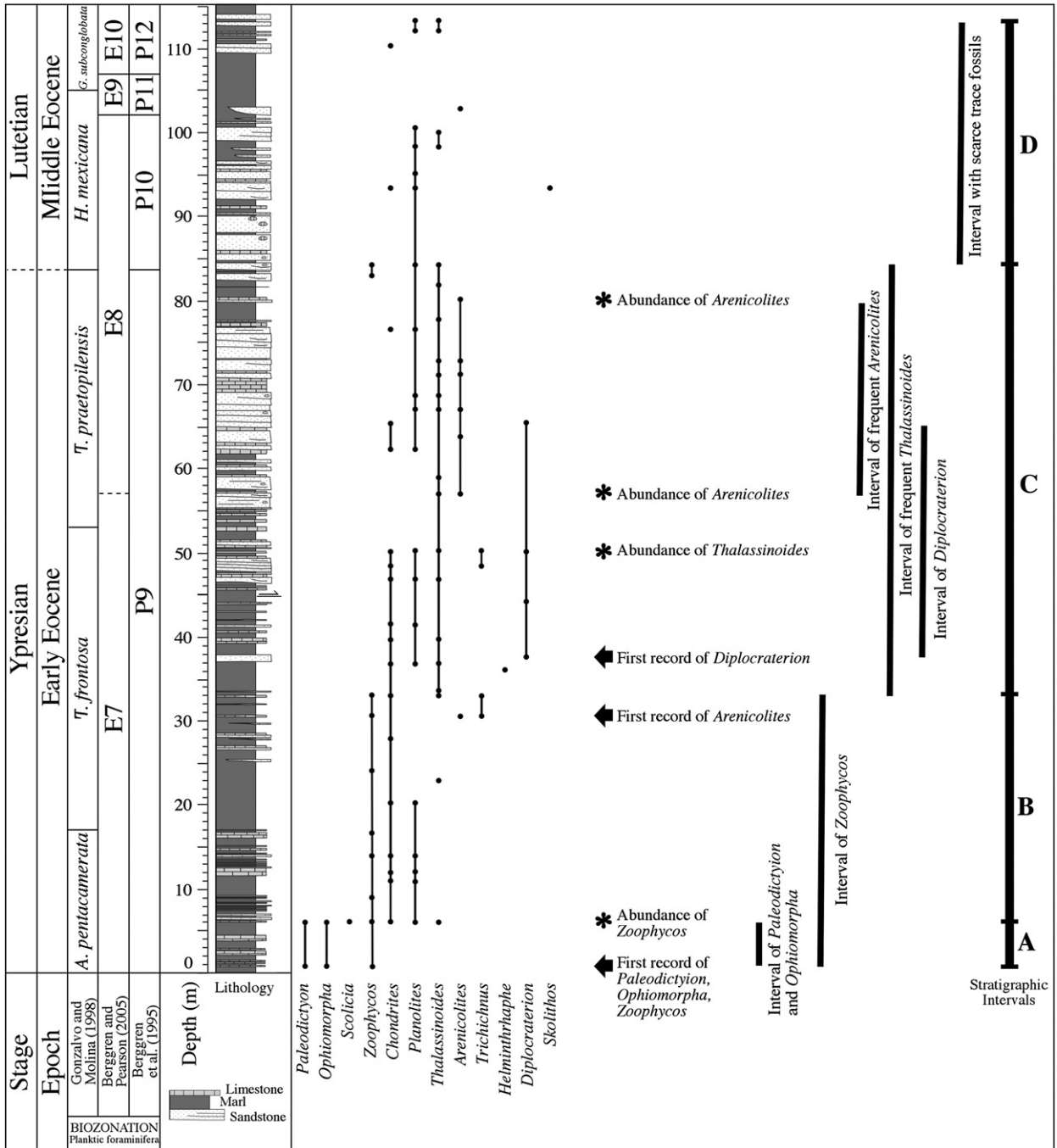


Fig. 5. Occurrence of trace fossils across the Ypresian–Lutetian transition at the Agost section, and the intervals (A–D) differentiated on the basis of trace fossils.

no longer dominated by illite and illitic mixed-layered illite-smectite. Moreover, the chlorite content decreases about meter 40. This boundary coincides with the end of the deposition of thick marl beds.

We observed a major mineralogical boundary between meters 53.1 and 57.4. Above this boundary the amount of total clay, quartz, and feldspars strongly decreases and palygorskite disappears completely while the amount of calcite strongly increases. Just below this boundary we found a strong increase

in the amount of dolomite and ankerite. This boundary coincides with the near complete end of the sedimentation of marls in that part of the section.

We assume that a subtle mineralogical boundary occurs between meters 79 and 80.5, above which the mixed-layered illite–smectites predominantly become very smectitic and chlorite seems to be more generally present. We observed a second major mineralogical boundary between meters 95.7 and 102. Above this boundary the clay mineralogy is dominated by

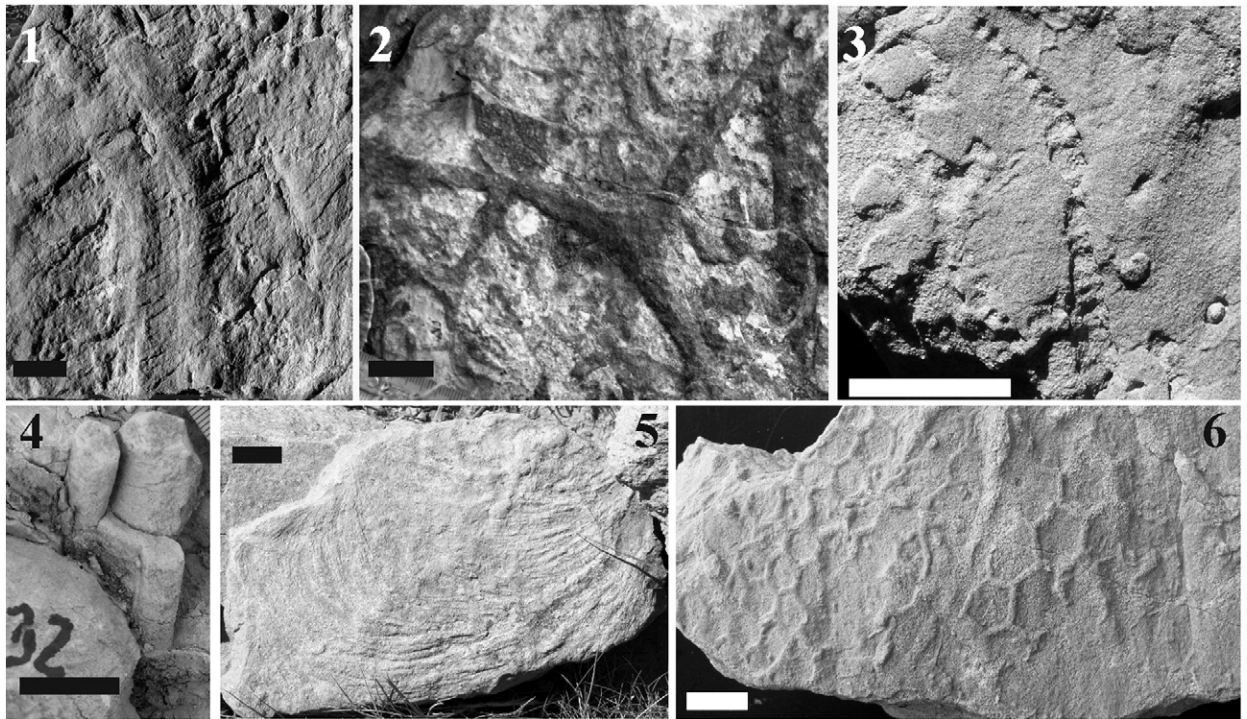


Plate I. Ichnotaxa from the Ypresian–Lutetian transition at the Agost section. Scale bar 2 cm. 1. *Scolicia*, specimen (meter 6). 2. *Thalassinoides*, specimen (meter 51). 3. *Ophiomorpha*, specimen (meter 5.5). 4. *Diplocraterion*, specimen (meter 37). 5. *Zoophycos*, specimen (meter 6). 6. *Paleodictyon*, specimen (meter 6).

almost pure smectites, palygorskite reappears, and kaolinite almost completely disappears. Also remarkable is the appearance of zeolites (probably clinoptilolite) in two samples also very rich in almost pure smectite. This last boundary marks the end of the deposition of thick sandstone beds and a renewed deposition of thick marl beds.

The association of palygorskite with illite and chlorite in the basal part of the section suggests a detrital origin rather than a climatic significance for palygorskite. The relationship of the different mineralogical boundaries with lithological facies changes, and in particular the association of more smectitic than illitic components with more sandy than marly sediments also suggests a change in provenance rather than changes in weathering conditions for the other boundaries. The association in the upper part of the section of almost pure smectite, palygorskite and some zeolites could point to neoformation of these minerals, maybe linked to volcanic glass alteration (especially smectite and zeolites) in evaporitic conditions.

4. Discussion

4.1. Palaeobathymetry

Benthic foraminiferal assemblages have been traditionally used as palaeobathymetric proxies (e.g., Bandy, 1960; Boltovskoy, 1978). The palaeodepth of the benthic foraminiferal assemblages is inferred from the bathymetric distribution of the individual species or genera reported for Palaeogene DSDP and ODP sites where palaeodepths can be derived independently by back-tracking (e.g., Tjalsma and Lohmann, 1983; Van

Morkhoven et al., 1986; Katz et al., 2003). Palaeodepth can also be inferred based upon comparisons between fossil and recent assemblages (e.g., Murray, 1991, 2006).

Benthic foraminiferal assemblages at the Agost section contain representatives of the Midway-type fauna described from the sublittoral Midway Formation in Texas (Berggren and Aubert, 1975). These fauna include such taxa as *Anomalinoidea acutus*, *Osangularia plummerae*, *Loxostomoides applini*, and several lagenids and polymorphinids. Moreover, other taxa common at sublittoral depths (e.g., asterigerinids, *Lobatula lobatula*, *Pararotalia audouini*) and the high influence of macrofauna are common at the Agost section. However, the common presence of the later, as well as of macroforaminifera, is probably related to transport by turbidity currents or by floating plant material. Species described from the cosmopolitan deep-bathyal Velasco Formation in Mexico (Berggren and Aubert, 1975), such as *Nuttallides truempyi* and *Bulimina trinitatensis*, are also recorded at the Agost section, but they are not common. Typical bathyal taxa such as *Hanzawaia ammophila*, *Cibicidoides eocaenus*, and buliminid species (*Bulimina semicostata*, *Buliminella grata*, *Buliminella beaumonti*, and *Bulimina alazanensis*) are abundant. Many of these bathyal species show a decrease in its relative abundance, or even they are not recorded, across the P9–P10 transition, and an increase in the upper part of the Agost section (Fig. 4).

Benthic foraminiferal assemblages suggest that sediments at the Agost section were deposited at upper-middle bathyal water depths but a relative sea-level fall is interpreted related to the P9–P10 transition.

In general, trace fossils suggest soft substrate and their assemblage can be interpreted in the context of softground

ichnofacies. Such ichnofacies are mainly differentiated according to depth-related ecological and sedimentary parameters (e.g., MacEachern et al., 2007 for an updated review). Usually the *Zoophycos* and the *Nereites* ichnofacies are related to deep-water environments, while the *Cruziana* ichnofacies characterizes shallow marine settings (MacEachern et al., 2007). The *Zoophycos* ichnofacies is traditionally viewed as being related to slopes below shelf while the *Nereites* ichnofacies is related to deeper environments. However, the bathymetric distribution of the *Zoophycos* ichnofacies can be wider and can embrace the outer shelf below the range of tempestites, slopes, abyssal plains, and pelagic highs. Thus, the *Zoophycos* ichnofacies can occur at the same or even greater depths than the *Nereites* ichnofacies, which can occur already below in the upper part of slope (Uchman et al., 2004; Uchman, 2006). Nevertheless, the succession *Nereites*–*Zoophycos*–*Cruziana* ichnofacies can be related to generally unidirectional change of bathymetry from bathyal, probably upper bathyal zone to sublittoral zone, to shallow circalittoral zone indicated by the *Cruziana* ichnofacies (Seilacher, 1967; Frey and Seilacher, 1980; Pemberton et al., 2001). Typically, the *Cruziana* ichnofacies is related to the zone below normal (fair weather) wave base and above stormwave base (Pemberton and MacEachern, 1995; Pemberton et al., 2001). The shallowing is accompanied by sedimentation change from proximal turbidites to immature gravity flow beds generated by storms.

Benthic foraminiferal and trace fossil assemblages show some discrepancies in our samples, but each indicates a decrease in palaeobathymetry throughout the Agost section. Benthic foraminifera suggest a decrease that occurs from upper-middle bathyal to sublittoral depths, while trace fossils suggest a decrease from upper bathyal–sublittoral to shallow circalittoral. However, benthic foraminiferal assemblages indicate a rapid recovery of water depth after the P9–P10 transition at the top of the section, while trace fossil assemblages, in contrast, indicate the continuity of circalittoral water-depths. These alternative interpretations are supported by the fact that benthic foraminiferal assemblages we studied from marls and trace fossil assemblages from sandstones.

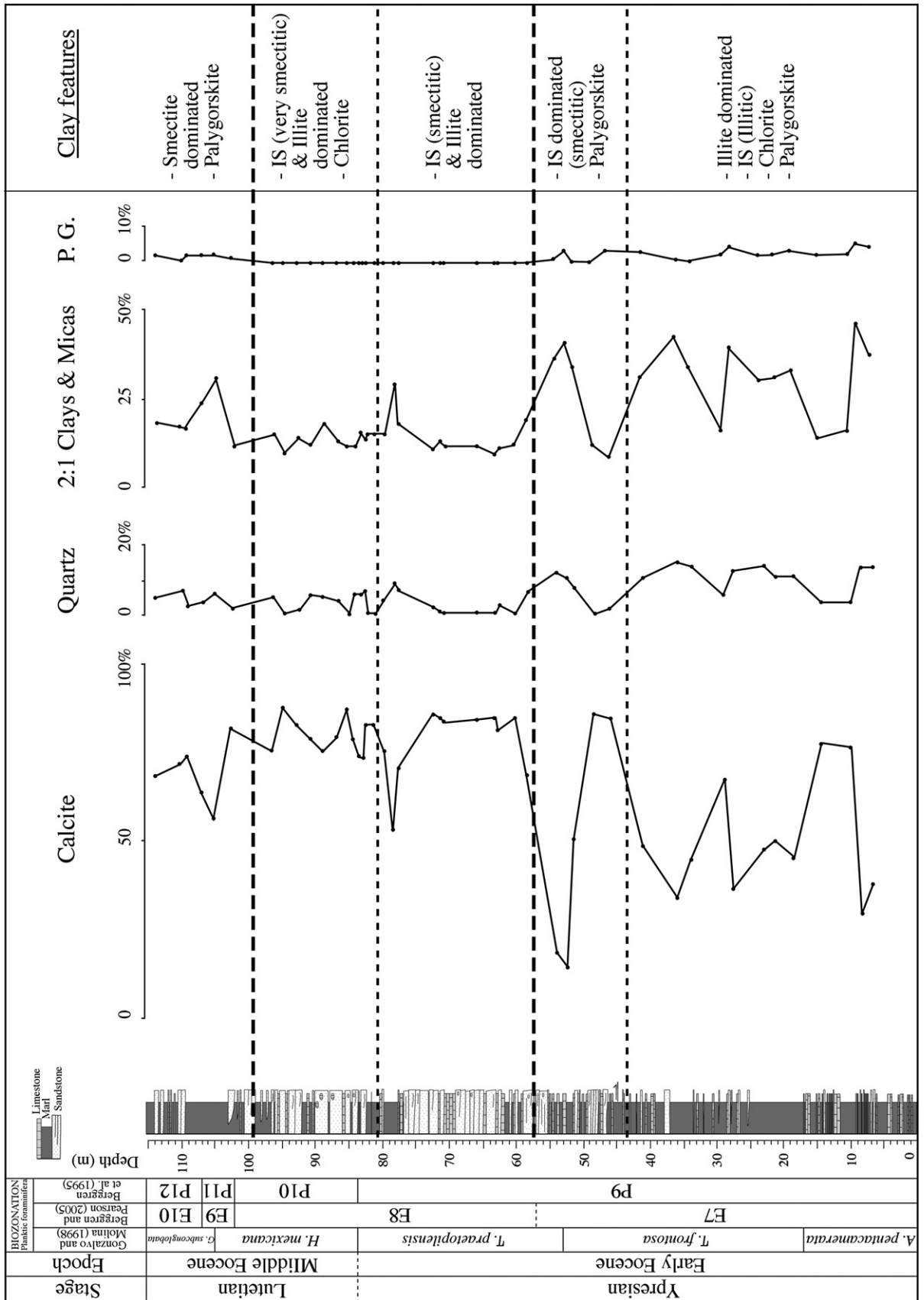
A major sea-level fall has been reported to be coeval with the base of the stratotype of the Lutetian Stage (Blondeau, 1981). Our results from both benthic foraminiferal and trace fossil assemblages suggest a significant sea-level change related to the P9–P10 transition.

4.2. Palaeoenvironmental turnover and implications for the Y/L boundary

Benthic foraminiferal assemblage composition is controlled by a number of strongly interdependent environmental parameters. However, the flux of organic matter to the deep sea-floor seems to be the main parameter structuring the assemblage (e.g., Jorissen et al., 2007), while both quantity and quality of organic matter seems to be causal ecological parameters (e.g., Fontanier et al., 2002, 2005). Lateral advection, either by intermediate or deep water currents, or by slope failure and turbidity currents, is a major factor responsible for the transport of particulate organic carbon to the ocean floor, often aged, i.e., refractory organic matter (e.g., Antia et al., 1999). Refractory organic matter is remineralized by anaerobic bacterial stocks in the dysaerobic ecosystems

deeper in the sediment, which could explain the high abundance of bolivinids at the Agost section. This low-quality organic matter has probably been supplied by turbidity currents, which are also responsible for the high abundance of the other main groups. *Cibicides* spp., *Lobatula lobatula*, and *Angulogerina muralis* characterized proximal settings under the influence of turbidity currents (Mackensen et al., 1995; Altenbach et al., 1999). Asterigerinids are probably allochthonous, which raises the problem of using benthic foraminiferal assemblages as a proxy for past currents. Active currents may constitute one of the main taphonomical factors, since they can winnow or add components to the original assemblages (Jorissen et al., 2007).

The most distinct peak in relative abundance of benthic foraminifera was that of *Aragonia aragonensis* at meter 86 which is located above the P9/P10 boundary where diversity values show a minimum. *Aragonia aragonensis* has been speculated to be to be an opportunistic species (Steineck and Thomas, 1996). This species shows peaks in relative abundance at several deep-ocean sites in the lowermost Eocene, just after the benthic foraminiferal extinction at the Paleocene/Eocene boundary (Thomas, 1990; Thomas and Zachos, 2000; Thomas et al., 2000) and at the Y/L boundary (Ortiz and Thomas, 2006), where it has been related to hyperthermal events. These early Eocene events resemble the PETM, but are less severe. They were marked by isotope anomalies, small individuals, low diversity and high dominance faunas (Lourens et al., 2005). Dominating taxa were *Nuttallides truempyi* and abyssaminids. The later may be opportunistic taxa colonizing a disturbed environment (Thomas and McCarren, 2005). At the Agost section, *N. truempyi* is not abundant and it is even not recorded across the P9/P10 boundary. The low abundance of *N. truempyi* is probably due to the inferred sea level change associated to the P9–P10 transition. Benthic foraminifera are a low-diversity fauna through the P9/P10 boundary interval but they also show similar minimum values in other parts of the section. The peak of *A. aragonensis* is not as distinct as in other sections but the occurrence of planktic foraminifera *Clavigerinella eocaenica* and *Clavigerinella jarvisi* at meter 81.7 (Fig. 7), and of warm-water calcareous nannofossils taxa such as *Sphenolithus*, *Discoaster barbadensis*, and *Ericsonia formosa*, just before the first occurrence of hantkeninids, provide compelling evidence for an excursion of tropical species due to an increase in seawater temperature (Larrasoña et al., in press). It has been also recorded related to the P9/P10 boundary an increase in pentoliths (calcareous nannofossils), which are indicators of low salinity and high nutrient conditions (Bukry, 1974; Kelly et al., 2003), together with a significant increase in the number of turbidite levels in the section between meters 81.7 and 86, suggesting enhanced continental weathering and run-off (Larrasoña et al., in press). A subtle mineralogical boundary is assumed between meters 79 and 80.5, above which the mixed-layered illite–smectites predominantly become very smectitic and chlorite seems to be more generally present. Chlorite is generally indicative of cold or dry conditions, while more smectitic minerals mean more intense weathering. However, these minerals probably suggest a change in provenance rather than changes in weathering conditions. Although pentoliths are indicative of high nutrient conditions, benthic foraminifera do not indicate higher flux of organic matter to the sea floor during this interval, since common eutrophic indicators such



as buliminid species (Thomas, 1998; Thomas and Röhl, 2002) show minimum values. Epifaunal morphogroups also show a slight increase.

A long stepped cooling trend through the middle and late Eocene followed the EECO (e.g., Zachos et al., 2001). However, another transient warming event has been identified at middle Eocene in Southern Ocean deep-sea cores (ca. 41.5 Ma), the middle Eocene climatic optimum (MECO) (Bohaty and Zachos, 2003). This warming event is characterized by a negative oxygen isotope anomaly but it lacks a significant negative carbon isotope excursion. Recently, the MECO has been recorded in the northern hemisphere in the Scaglia limestones of the Contessa Highway section of central Italy ca. 40 Ma (Jovane et al., 2007), indicating that long-term cooling through the middle and late Eocene was not monotonic. These events are all recorded at more than 800–1000 m water depth. Moreover, shallow settings were less affected than deep ones during the PETM (e.g., Alegret et al., 2005). Thus, a hyperthermal event could have occurred during the Y–L transition, but the upper-middle bathyal Agost section is probably not deep enough to record all the signs that characterize a hyperthermal event, which is indeed recorded at the Agost section water column by planktic foraminifera and calcareous nanofossils. In addition, it is not clear if these events were formed as a result of greenhouse gas input (carbon isotope excursion), or whether they reflect the cumulative effects of periodic changes in ocean chemistry and circulation (e.g., Kroon et al., 2007).

Larrasoña et al. (in press) suggested that the FO of *Blackites inflatus* (base of CP12b) might be chosen as the primary marker for the Y/L boundary. The basis for their argument is that *B. inflatus* FO is the only biostratigraphic event which is synchronous and well represented in most of the sections where reliable magnetobiostratigraphic results have been obtained (Bernaola et al., 2006; Payros et al., 2007). It is found within Chron C21r (Fig. 7) which conforms to the magnetostratigraphically calibrated age of ca. 48 Ma (middle part of C21r) that is considered in standard calibration schemes (e.g., Berggren et al., 1995; Berggren & Pearson 2005, 2006; Pearson et al., 2006). Benthic foraminiferal assemblages show a distinct decrease in diversity, trace fossils change from the *Nereites* to *Zoophycos* ichnofacies, and mineralogical analyses do not indicate any distinct change related to the CP12a/CP12b boundary at the Agost section. Related to the other marker events traditionally used to define the Y/L boundary, trace fossils change from *Zoophycos* to *Cruziana* ichnofacies at the SBZ12/SBZ13 boundary (meter 34), and a major mineralogical boundary occurs close to the E8/E9 boundary (meter 57) which coincides with the near complete end of the sedimentation of marls in that part of the section (Fig. 7).

5. Conclusions

Our analysis of the quantitative stratigraphic distribution of benthic and planktic foraminiferal assemblages, and characterization of trace fossil assemblages, integrated with

mineralogical analyses, permits a palaeoenvironmental interpretation for the Y–L transition at the Agost section. Benthic foraminiferal and trace fossil assemblages are highly influenced by turbidity currents and other gravity currents which probably added refractory organic matter to the sea floor. This pattern underscores the importance of the quality of organic matter as a main factor structuring benthic assemblages in the past. However, integrated study of benthic foraminiferal and trace fossil assemblages allows inference regarding the upper to middle bathyal palaeodepths for the lower part of the Agost section, and a change to sublittoral to circalittoral palaeodepths related to the P9–P10 transition. The shallowing is accompanied by sedimentation change from proximal turbidites to immature gravity flow beds generated by storms.

Mineralogical changes across the Agost section seem to be related to the lithological variations in the section rather than to climatic changes. However, it should be kept in mind that warmer or drier conditions may be indicated at the topmost part of the section.

Several marker events such as the peak of *Aragonia aragonensis* abundance and the co-occurrence across a short-interval of time of *Clavigerinella eoacena* and *Clavigerinella jarvisi* and warm-water calcareous nanofossils, suggest a transient warm event or hyperthermal event related to the FO of hantkeninids, i.e., the P9/P10 boundary. This event could be a good criterion to enable widespread recognition of the base of the Lutetian Stage in support or in the absence of the primary marker if the FO of hantkeninids were selected as the primary marker. Nevertheless, this event should be further studied in deep marine successions and in other palaeobathymetric settings in order to test whether it represents a global event that could be used for worldwide correlation of the Y/L boundary. Besides, the FO of the calcareous nanofossil *Blackites inflatus* (base of CP12b) is a synchronous event and well represented in most sections where reliable magnetobiostratigraphic results have been obtained. Thus, our data integrated with those of Larrasoña et al. (in press) point to the FO of hantkeninids (base of P10) or the FO of *B. inflatus* (base of CP12b), 3–5 Myr before the P9/P10 boundary, as the most suitable primary marker events to define the GSSP for the base of the Lutetian Stage. Whatever the marker event chosen, all the successive events recognized at the Agost section allow a complete characterization of the Y–L transition. Thus the Agost section may be a suitable candidate to locate the GSSP for the Y/L boundary.

Acknowledgements

We thank H.P. Luterbacher, K. Olsson, and an anonymous reviewer for constructive reviews of earlier manuscript. This research was funded by the CGL 2007–63724 Consolider Project (Spanish Ministry of Education and Science). S. Ortiz thanks the Spanish Ministry of Education and Science for the postdoctoral grant EX2007–1094. The research of F.J. Rodríguez-Tovar was supported by project CGL2005–01316/BTE and the RNM–178 group. A. Uchman got additional support from the Jagiellonian

Fig. 6. Graphic representation of the weight percentages of the most important minerals and mineral groups based on the data in Appendix B.3. The column on the right summarizes the most important features of the qualitative clay mineralogy. ("2:1 dioctahedral clays and micas" = illite/smectite/illite-smectite/micas; "P.G." = palygorskite; "IS" = illite-smectite). Mineralogical boundaries are indicated in dashed lines.

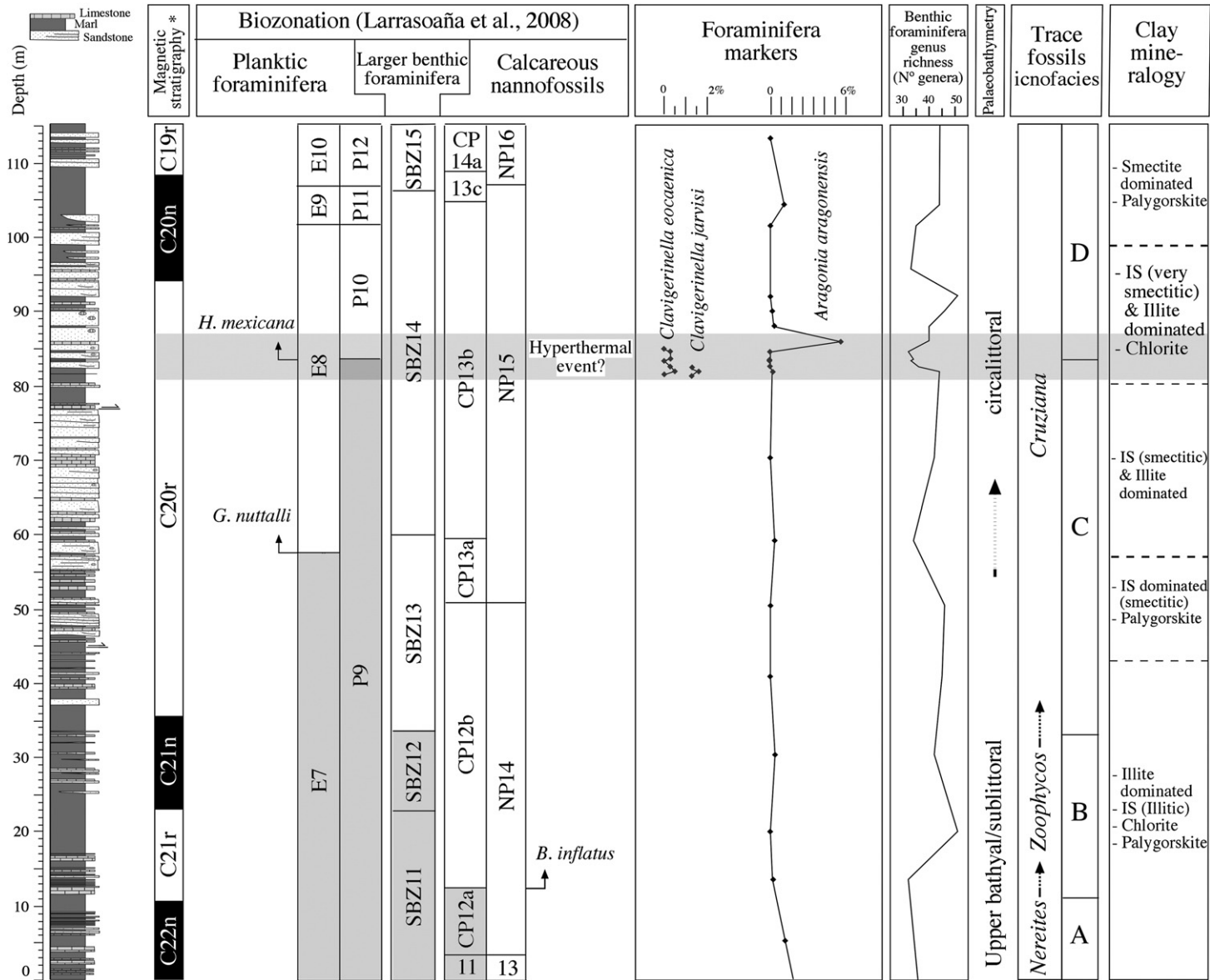


Fig. 7. Integration of the most representative data from the Agost section indicating the extent of the possible hyperthermal event. The grey bars indicate the position of the Ypresian according to different fossil groups, i.e., the Ypresian/Lutetian boundary. *Magnetic stratigraphy developed by Larrasoña et al. (in press).

University (DS 812 funds). E. Zeelmaekers wishes to thank the Institute for the Promotion of Innovation through Science and Technology in Flanders (IWT-Vlaanderen) and Chevron ETC and Douglas K McCarty in particular for permitting to use the QUANTA proprietary software.

Appendix A. Taxonomic list and original references of the benthic and planktic foraminiferal species and trace fossil species identified in the Ypresian–Lutetian transition at the Agost section

Planktic foraminifera

Acarinina bullbrooki (Bolli) 1957 = *Globorotalia bullbrooki* Bolli 1957, p. 167, pl. 38, figs. 4a–c, 5a–c.

Acarinina cuneicamerata (Blow) 1979 = *Globorotalia (Acarinina) cuneicamerata* Blow 1979, p. 924–926, pl. 146, figs. 6–8; pl. 148, figs. 4–6; pl. 153, figs. 1–4; pl. 156, figs. 1–4; pl. 165, figs. 4, 7; pl. 203, fig. 5.

Acarinina matthewsae Blow 1979 = *Globorotalia (Acarinina) matthewsae* Blow 1979, p. 935–937, pl. 170, figs. 1–9; pl. 179, figs. 1, 2; pl. 187, fig. 5; pl. 203, figs. 3, 4; pl. 204, figs. 1–5; pl. 205, figs. 1–6.

Acarinina pentacamerata (Subbotina) 1947 = *Globorotalia pentacamerata* Subbotina 1947, p. 128–129, pl. 7, figs. 12–17.

Acarinina praetopilensis (Blow) 1979 = *Globorotalia (Truncorotaloides) topilensis* (Cushman) subsp. *praetopilensis* Blow 1979, p. 1043, pl. 155, fig. 9; pl. 203, figs. 1–2; pl. 169, figs. 1–9; pl. 207, figs. 1, 2; pl. 208, figs. 1–4; pl. 208, Fig. 5; pl. 178, figs. 6–9; pl. 185, figs. 7–8; pl. 187, figs. 1–2; pl. 208, Fig. 6; pl. 187, figs. 3–4.

Acarinina primitiva (Finlay, 1947) = *Globoquadrina primitiva* Finlay 1947, p. 291, pl. 8, figs. 129–134.

Acarinina pseudotopilensis Subbotina 1953, p. 227, pl. 21, figs. 8a–c, 9a–c; pl. 22, figs. 1a–3c.

Acarinina topilensis (Cushman) 1925 = *Globigerina topilensis* Cushman 1925, p. 7, pl. 1, figs. 9a–c.

Acarinina rohri Brönnimann and Bermudez 1953, p. 818–819, pl. 87, figs. 7–9.

Acarinina soldadoensis (Brönnimann) 1952 = *Globigerina soldadoensis* Brönnimann 1952, p. 9, 7, pl. 1, figs. 1–9.

Clavigerinella eocanica (Nuttall) 1928 = *Hastigerinella eocanica* Nuttall 1928, p. 376, pl. 50, figs. 9–11.

Clavigerinella jarvisi (Cushman) 1930 = *Hastigerinella jarvisi* Cushman 1930, p. 18, pl. 3, fig. 8.

Globigerinatheka index (Finlay) 1939 = *Globigerinoides index* Finlay 1939, p. 125, pl. 14, figs. 85–88.

Globigerinatheka mexicana (Cushman) 1925 = *Globigerina mexicana* Cushman 1925, p. 61, pl. 1, figs. 8a–b.

Globigerinatheka subconglobata (Shutskaya) 1958 = *Globigerinoides subconglobatus* Shutskaya var. *subconglobatus* Shutskaya 1958, p. 86, pl. 1, figs. 4–11.

Globigerinoides rubrififormis Subbotina 1953, p. 92, pl. 13, fig. 19a–b; pl. 14, figs. 6–9.

Specimens arranged in a high trochospire, with well-defined incised sutures and large, high-arched, primary aperture are included.

Guembeltrioides nuttalli (Hamilton) 1953 = *Globigerinoides nuttalli* Hamilton 1953, p. 224–225, pl. 32, figs. 22–24.

Hantkenina dumblei Weinzierl and Applin 1929 = *Hantkenina dumblei* Weinzierl and Applin, p. 402, pl. 43, figs. 5a–b.

Hantkenina mexicana Cushman 1924 = *Hantkenina mexicana* Cushman 1924, p. 3, pl. 2, fig. 2.

Hantkenina nuttalli (Toumarkine) 1981 = *Hantkenina nuttalli* Toumarkine, p. 112, pl. 1, fig. 4–6 (fig. 4 from Nuttall, 1930, pl. 24, fig. 3 paratype of *H. mexicana* var. *aragonensis*; fig. 5 and 6 from Nuttall, 1930 redrawn in Bolli et al., 1957).

Hantkenina cf. *singanoae* Pearson and Coxall 2006, p. 252, pl. 8.13, figs. 1–17.

Igorina broedermanni (Cushman and Bermudez) 1949 = *Globorotalia (Truncorotalia) broedermanni* Cushman and Bermudez 1949, p. 40, pl. 7, figs. 22–24.

Morozovella aragonensis (Nuttall) 1930 = *Globorotalia aragonensis* Nuttall 1930, p. 288, pl. 24, figs. 6–8, 10–11.

Morozovella caucasica (Glaessner) 1937 = *Globorotalia aragonensis* var. *caucasica* Glaessner 1937, p. 31, pl. 1, figs. 6a–c.

Morozovella dolabrata (Jenkins) 1965 = *Globorotalia dolabrata* Jenkins 1965, p. 1113, pl. 10, figs. 104–112.

Morozovella hungarica (Samuel) 1972 = *Globorotalia hungarica* Samuel 1972, p. 191, 192, pl. 50, figs. 2–5.

Morozovelloides lehneri (Cushman and Jarvis) 1929 = *Globorotalia lehneri* Cushman and Jarvis 1929 p. 17, pl. 3, figs. 16a–c.

Morozovella spinulosa (Cushman) 1927 = *Globorotalia spinulosa* Cushman 1927, p. 114, pl. 23, figs. 4a–c.

Parasubbotina griffinae (Blow) 1979 = *Globorotalia (Turborotalia) griffinae* Blow, p. 1072, pl. 96, figs. 5–9pl.150, figs. 5–9; pl. 157, fig. 7; pl. 162, figs. 8, 9; pl. 165, figs. 1–3.

Pseudohastigerina micra (Cole) 1927 = *Nonion micrus* Cole 1927, p. 22, pl. 5, fig. 12.

Subbotina boweri (Bolli) 1957 = *Globigerina boweri* Bolli 1957, p. 163, pl. 36, figs. 1–2.

Subbotina inaequispira (Subbotina) 1953 = *Globigerina inaequispira* Subbotina 1953, p. 69, pl. 6, figs. 1–4.

Pseudoglobigerinella bolivariana (Petters) 1954 = *Globigerina wilsoni* Cole subsp. *bolivariana* Petters 1954, p. 39, pl. 8, fig. 9a–c.

Turborotalia frontosa (Subbotina, 1953) = *Globigerina frontosa* Subbotina 1953, p. 84, pl. 12, figs. 3a–c, 4a–c, 6a–7c.

Benthic foraminifera

Alabamina wilcoxensis Toulmin 1941, p. 603, pl. 81, figs. 10–14; textfig. 4A–C.

Angulogerina muralis (Terquem) 1882 = *Uvigerina muralis* Terquem 1882, p. 119, pl. 12, figs. 26–29.

Anomalinoides acutus (Plummer) = *Anomalina ammonoides* (Reuss) var. *acuta* Plummer 1926, p. 149, pl. 10, fig. 2a–c.

Aragonia aragonensis (Nuttall) 1930 = *Textularia aragonensis* Nuttall 1930, p. 280, pl. 23, fig. 6.

Bolivinooides crenulata (Cushman) 1936 = *Bolivina crenulata* Cushman 1936, p. 50, pl. 7, fig. 13

Bulimina alazanensis Cushman 1927, p. 161, pl. 25, fig. 4.

Bulimina mexicana Cushman 1922 = *Bulimina inflata* Seguenza var. *mexicana* Cushman 1922, p. 95, lám. 21, fig. 2.

Bulimina aff. *midwayensis* Cushman and Parker = *Bulimina ardelphiana* Cushman and Parker var. *midwayensis* Cushman and Parker 1936, p. 42, pl. 7, figs. 9 and 10.

Bulimina semicostata Nuttall 1930, p. 285, pl. 23, figs. 15, 16.

Bulimina trinitatensis Cushman and Jarvis 1928, p. 102, pl. 14, fig. 12.

Bulminella beaumonti Cushman and Renz 1946, p. 36, pl. 6, fig. 7.

Bulminella grata Parker and Bermudez 1937, p. 515, pl. 59, fig. 6a–c.

Cibicides westi Howe 1939, p. 88, pl. 13, figs. 20–22.

Cibicoides eocaenus (Gümbel) 1868 = *Rotalia eocaena* Gümbel 1868, p. 650, pl. 2, fig. 87.

Cibicoides hadjibulakensis Bykova 1954 = *Cibicides* (*Cibicoides*) *hadjibulakensis* Bykova en Vasilenko, 1954, p. 177, pl. 31, fig. 5

Cibicoides naranjoensis (White) 1928 = *Cibicides naranjoensis* White 1928, p. 298, pl. 41, fig. 1.

Cibicoides propius Brotzen 1948, p. 78, pl. 12, figs. 3, 4.

Clavulinoides angularis (d'Orbigny) 1826 = *Clavulina angularis* d'Orbigny 1826, p. 268, pl. 12, fig. 7.

Globocassidulina subglobosa (Brady) 1881 = *Cassidulina subglobosa* Brady, 1881, p. 60 (type reference). Brady 1884, p. 430, lám. 54, fig. 17 (type figure).

Hanzawaia ammophila (Gümbel) 1868 = *Rotalia ammophila* Gümbel 1868, p. 652, pl. 2, fig. 90.

Lobatula lobatula (Walker and Jacob) 1798 = *Nautilus lobatulus* Walker and Jacob 1798, p. 20, pl. 3, fig. 71.

Loxostomoides applini (Plummer) 1926 = *Bolivina applini* Plummer 1926, p. 69, pl. 4, fig. 1.

Nuttallides truempyi (Nuttall) = *Eponides truempyi* Nuttall 1930, p. 287, pl. 24 figs. 9, 13, 14.

Osangularia plummerae Brotzen 1940, p. 30, textfig. 8.

Turrilina brevispira Ten Dam 1944, p. 110, pl. 3, fig. 14.

Trace fossil

Ophiomorpha annulata (Książkiewicz) 1977

Ophiomorpha rudis (Książkiewicz) 1977

Appendix B. Supplementary data

Supplementary data associated with this article can be found, in the online version, at doi:10.1016/j.marmicro.2008.09.001.

References

- Alegret, L., Ortiz, S., Arenillas, I., Molina, E., 2005. Paleoenvironmental turnover across the Paleocene/Eocene Boundary at the Stratotype section in Dababiya (Egypt) based on benthic foraminifera. *Terra Nova* 7, 526–536.
- Alonso-Zarza, A.M., Armenteros, A., Braga, J.C., Muñoz, A., Pujalte, V., Ramos, E., Aguirre, J., Alonso-Gavilán, G., Arenas, C., Baceta, J.I., Carballeira, J., Calvo, J.P., Corrochano, A., Fornós, J.J., González, A., Luzón, A., Martín, J.M., Pardo, G., Payros, A., Pérez, A., Pomar, L., Rodríguez, J.M., Villena, J., 2002. Tertiary. In: Gibbons, W., Moreno, T. (Eds.), *The Geology of Spain*. Geological Society, London, pp. 293–334.
- Altenbach, A.V., Pflaumann, U., Schiebel, R., Thies, A., Timm, S., Trauth, M., 1999. Scaling percentages and distributional patterns of benthic foraminifera with flux rates of organic carbon. *Journal of Foraminiferal Research* 29, 173–185.
- Antia, A.N., Von Bodungen, B., Peinert, R., 1999. Particle flux across the mid-European continental margin. *Deep-Sea Research* 46, 1999–2024.
- Bandy, O.L., 1960. General correlation of foraminiferal structure with environment. Report of the International Geological Congress, 21st Session, Copenhagen, Pt. vol. 22, pp. 7–19.
- Berggren, W.A., Aubert, J., 1975. Paleocene benthonic foraminiferal biostratigraphy, paleobiogeography and paleoecology of Atlantic–Tethyan regions: midway-type fauna. *Palaeogeography, Palaeoclimatology, Palaeoecology* 18, 73–192.
- Berggren, W.A., Pearson, P.N., 2005. A revised tropical to subtropical Paleogene planktonic foraminiferal zonation. *Journal of Foraminiferal Research* 35, 279–298.
- Berggren, W.A., Pearson, P.N., 2006. Tropical to subtropical planktonic foraminiferal zonation of the Eocene and Oligocene. In: Pearson, P.N., Olsson, R.K., Huber, B.T., Hemleben, C., Berggren, W.A. (Eds.), *Atlas of Eocene planktonic foraminifera*. Cushman Foundation Special Publication, vol. 41, pp. 29–40.
- Berggren, W.A., Kent, D.V., Swisher, C.C., Aubry, M.-P., 1995. A revised Cenozoic geochronology and chronostratigraphy. In: Berggren, W.A., Kent, D.V., Hardenbol, J. (Eds.), *Geochronology, Time Scales and Global Stratigraphic Correlations: A Unified Temporal Framework for an Historical Geology*. Society of Economic Paleontologists and Mineralogists Special Publication, vol. 54, pp. 129–212. Tulsa, OK.
- Bernaola, G., Orue-Etxebarria, X., Payros, A., Dinarès-Turell, J., Tosquella, J., Apellaniz, E., Caballero, F., 2006. Biomagnetostratigraphic analysis of the Gorrondatxe section (Basque Country, Western Pyrenees): its significance for the definition of the Ypresian/Lutetian boundary stratotype. *Neues Jahrbuch für Geologie und Paläontologie Abhandlungen* 241, 67–109.
- Bernhard, J.M., 1986. Microaerophilic and facultative anaerobic benthic foraminifera: a review of experimental and ultrastructural evidence. *Revue de Paléobiologie* 15, 261–275.
- Bernhard, J.M., Sen Gupta, B.K., 1999. Foraminifera of oxygen-depleted environments. In: Sen Gupta, B.K. (Ed.), *Modern foraminifera*. Kluwer, Dordrecht, Netherlands, pp. 201–216.
- Blondeau, A., 1981. Lutetian. *Bulletin d'Information des Géologies du Bassin de Paris* 2, 167–180.
- Bohaty, S.M., Zachos, J.C., 2003. Significant Southern Ocean warming event in the late middle Eocene. *Geology* 31, 1017–1020.
- Boltovskoy, E., 1978. La distribución batimétrica de los foraminíferos bentónicos. *Ameghiniana* 15, 409–421.
- Bukry, D., 1974. Coccoliths as paleosalinity indicators; evidence from Black Sea. *American Association of Petroleum Geologists Memoir* 20, 353–363.
- Buzas, M.A., Culver, S.J., Jorissen, F.J., 1993. A statistical evaluation of the microhabitats of living (stained) infaunal benthic foraminifera. *Marine Micropaleontology* 20, 311–320.
- Corliss, B.H., 1985. Microhabitats of benthic foraminifera within deep-sea sediments. *Nature* 314, 435–438.
- Corliss, B.H., Chen, C., 1988. Morphotype patterns of Norwegian Sea deep-sea benthic foraminifera and ecological implications. *Geology* 16, 716–719.
- Fontanier, C., Jorissen, F.J., Licari, L., Alexandre, A., Anschutz, P., Carbonel, P., 2002. Live benthic foraminiferal faunas from the Bay of Biscay: faunal density, composition and microhabitats. *Deep-Sea Research* 49, 751–785.
- Fontanier, C., Jorissen, F.J., Chaillou, G., Anschutz, P., Gremare, A., Grivaud, C., 2005. Foraminiferal faunas from a 2800 deep lower canyon station from the Bay of Biscay: faunal response to focusing of refractory organic matter. *Deep-Sea Research* 52, 1189–1227.
- Frey, R.W., Seilacher, A., 1980. Uniformity in marine invertebrate ichnology. *Lethaia* 13, 183–207.
- Goody, A.J., 1994. The biology of deep-sea foraminifera: a review of some advances and their applications in paleoceanography. *Palaios* 9, 14–31.
- Gonzalvo, C., Molina, E., 1998. Planktic foraminiferal biostratigraphy across the Lower–Middle Eocene transition in the Betic Codillera (Spain). *Neues Jahrbuch für Geologie und Paläontologie Monatshefte* 11, 671–693.
- Jackson, M.L., 1975. Soil chemical analysis – Advanced course, 2de editie. Published by the author, Madison, Wisconsin.
- Jones, R.W., Charnock, M.A., 1985. “Morphogroups” of agglutinated foraminifera. Their life positions and feeding habits and potential applicability in (paleo)ecological studies. *Revue de Paléobiologie* 4, 311–320.
- Jorissen, F.J., De Stigter, H.C., Widmark, J.G.V., 1995. A conceptual model explaining benthic foraminiferal microhabitats. *Marine Micropaleontology* 26, 3–15.
- Jorissen, F.J., Fontanier, C., Thomas, E., 2007. Paleoclimatological proxies based on deep-sea benthic foraminiferal assemblage characteristics. In: Hillaire-Marcel, C., de Vernal, A. (Eds.), *Proxies in Late Cenozoic Paleoclimatology* (Pt. 2): Biological tracers and biomarkers, Elsevier, location.
- Jovane, L., Florindo, F., Coccioni, R., Dinarès-Turell, J., Marsili, A., Monechi, S., Roberts, A.P., Sprovieri, M., 2007. The middle Eocene climatic optimum event in the Contessa Highway section, Umbrian Apennines, Italy. *Geological Society of America Bulletin* 119, 413–427.
- Katz, M.E., Tjalsma, R.C., Miller, K.G., 2003. Oligocene bathyal to abyssal benthic foraminifera of the Atlantic Ocean. *Micropaleontology* 49, 1–45.
- Kelly, D.C., Norris, R.D., Zachos, J.C., 2003. Deciphering the paleoceanographic significance of Early Oligocene Braarudosphaera chalks in the South Atlantic. *Marine Micropaleontology* 49, 49–63.
- Kroon, D., Zachos, J.C., Leg 208 Scientific Party, 2007. Leg 208 synthesis: Cenozoic climate cycles and excursions. In: Kroon, D., Zachos, J.C., Richter, C. (Eds.), *Proc. ODP, Sci. Results*, vol. 208. Ocean Drilling Program, College Station, TX, pp. 1–55.
- Lapparent, A.D., 1883. *Traité de Géologie* Paris. Paris, Savy.

- Larrasoña, J.C., Gonzalvo, C., Molina, E., Monechi, S., Ortiz, S., Tori, F., Tosquella, J., in press. Integrated magnetobiochronology of the Early/Middle Eocene transition at Agost (Spain): implications for defining the Ypresian/Lutetian boundary stratotype. *Lethaia*. doi:10.1111/j.1502-3931.2008.00096.x.
- Loeblich, A.R., Jr., Tappan, H., 1988. Foraminiferal Genera and Their Classification. Van Nostrand Reinhold Company (Ed.), 2 vol.
- Lourens, L.J., Sluijs, A., Kroon, D., Zachos, J.C., Thomas, E., Röhl, U., Bowles, J., Raffi, I., 2005. Astronomical pacing of late Palaeocene to early Eocene global warming events. *Nature* 435, 1083–1087.
- Lowrie, W., Alvarez, W., Napoleone, G., Perch-Nielsen, K., Premoli Silva, I.P., Toumarkine, M., 1982. Paleogene magnetic stratigraphy in Umbrian pelagic carbonate rocks – the Contessa sections, Gubbio. *Geological Society of America Bulletin* 93, 414–432.
- Luterbacher, H.P., Alli, J.R., Brinkhuis, H., Gradstein, F.M., Hooker, J.J., Monechi, S., Ogg, J.G., Powell, J., Röhl, U., Sanfilippo, A., Schmitz, B., 2004. The Paleogene period. In: Gradstein, F.M., Ogg, J.G., Smith, A.G. (Eds.), *A Geologic Time Scale 2004*. Cambridge University Press, pp. 384–408.
- Lutze, G.F., Altenbach, A., 1988. *Rupertina stabilis* (Wallich), a highly adapted, suspension feeding foraminifer. *Meyniana* 40, 55–69.
- MacEachern, J.A., Pemberton, S.G., Gingras, M.K., Bann, K.L., 2007. The ichnofacies paradigm: a fifty-year retrospective. In: Miller III, W. (Ed.), *Trace Fossils. Concepts, Problems, Prospects*. Elsevier, Amsterdam, pp. 52–77.
- Mackensen, A., Schmiedl, G., Harloff, J., Giese, M., 1995. Deep-sea foraminifera in the South Atlantic Ocean: ecology and assemblage generation. *Micropaleontology* 41, 342–358.
- Martín-Algarra, L., Vera, J.A., 2004. La Cordillera Bética y las Baleares en el contexto del Mediterráneo Occidental. In: Vera, J.A. (Ed.), *Geología de España*. SGE-IGME, Madrid, pp. 352–354.
- Molina, E., Cosovic, V., Gonzalvo, C., Von Salis, K., 2000. Integrated biostratigraphy across the Ypresian/Lutetian boundary at Agost, Spain. *Revue de Micropaléontologie* 43, 381–391.
- Molina, E., Gonzalvo, C., Ortiz, S., Cruz, L.E., 2006. Foraminiferal turnover across the Eocene-Oligocene transition at Fuente Caldera, southern Spain: no cause-effect relationship between meteorite impacts and extinctions. *Marine Micropaleontology* 58, 270–286.
- Moore, D.M., Reynolds Jr., R.C., 1997. X-ray diffraction and the identification and analysis of clay minerals. Oxford University Press, Oxford-New York.
- Murray, J.W., 1991. Ecology and paleoecology of benthic foraminifera. Longman, Harlow.
- Murray, J.W., 2006. Ecology and Applications of Benthic Foraminifera. Cambridge University Press, Cambridge.
- Mystkowski, K., Środoń, J., McCarty, D.K., 2002. Application of evolutionary programming to automatic XRD quantitative analysis of clay-bearing rocks: The Clay Minerals Society 39th Annual Meeting, abstract, Boulder, Colorado.
- Napoleone, G., Premoli Silva, I., Heller, F., Cheli, P., Corezzi, S., Fischer, A.G., 1983. Eocene magnetic stratigraphy at Gubbio, Italy, and its implications for Paleogene geochronology. *Geological Society of America Bulletin* 94, 181–191.
- Okada, H., Bukry, D., 1980. Supplementary modification and introduction of code numbers to the low-latitude coccolith biostratigraphic zonation (Bukry, 1973; 1975). *Marine Micropaleontology* 5, 321–325.
- Omotoso, O., McCarty, D.K., Hillier, S., Kleeberg, R., 2006. Some successful approaches to quantitative mineral analysis as revealed by the 3rd Reynolds Cup Contest. *Clays and Clay Minerals* 54, 748–760.
- Ortiz, S., Thomas, E., 2006. Lower-middle Eocene benthic foraminifera from the Fortuna section (Betic Cordillera, southeastern Spain). *Micropaleontology* 52, 97–150.
- Payros, A., Bernaola, G., Orue-Etxebarria, X., Dinarès-Turell, J., Tosquella, J., Apellaniz, E., 2007. Reassessment of the Early–Middle Eocene biomagnetochronology based on evidence from the Gorrondatxe section (Basque Country, western Pyrenees). *Lethaia* 40, 183–195.
- Pearson, P.N., Olsson, R.K., Huber, B.T., Hemleben, C., Berggren, W.A. (Eds.), 2006. Atlas of Eocene Planktonic Foraminifera. Cushman Foundation Special Publication, vol. 41.
- Pemberton, S.G., MacEachern, J.A., 1995. The sequence stratigraphy significance of trace fossils: examples from the Cretaceous foreland basin of Alberta, Canada. In: Van Wagoner, J.C., Bertram, G. (Eds.), *Sequence stratigraphy of foreland basin deposits: outcrop and subsurface examples from the Cretaceous of North America*. American Association of Petroleum Geologists Memoirs, vol. 64, pp. 429–475. Tulsa, OK.
- Pemberton, G.S., Spila, M., Pulham, A.J., Saunders, T., MacEachern, J.A., Robbins, D., Sinclair, I.K., 2001. Ichnology and Sedimentology of shallow to marginal marine systems: Ben Nevis and Avalon Reservoirs, Jeanne D'Arc Basin. Geological Association of Canada, Short Course Notes, vol. 15.
- Remane, J., Bassett, M.G., Cowie, J.W., Gohrbandt, K.H., Lane, H.R., Michelsen, O., Naiwen, W., 1996. Revised guidelines for the establishment of global chronostratigraphic standards by the International Commission on Stratigraphy (ICS). *Episodes* 19, 77–81.
- Seilacher, A., 1967. Bathymetry of trace fossils. *Marine Geology* 5, 413–428.
- Serra-Kiel, J., Hottinger, L., Caus, E., Drobne, K., Ferrandez, C., Jauhri, A.K., Less, G., Pavlovec, R., Pignatti, J., Samso, J.M., Schaub, H., Sirel, E., Strougo, A., Tambareau, Y., Tosquella, J., Zakrevskaya, E., 1998. Larger foraminiferal biostratigraphy of the Tethyan Paleocene and Eocene. *Bulletin de la Societe Geologique de France* 169, 281–299.
- Schönfeld, J., 1997. The impact of the Mediterranean Outflow Water (MOW) on benthic foraminiferal assemblages and surface sediments at the southern Portuguese continental margin. *Marine Micropaleontology* 29, 211–236.
- Schönfeld, J., 2002a. Recent benthic foraminiferal assemblages in deep high-energy environments from the Gulf of Cadiz (Spain). *Micropaleontology* 44, 141–162.
- Schönfeld, J., 2002b. A new benthic foraminiferal proxy for near-bottom current velocities in the Gulf of Cadiz, northeastern Atlantic Ocean. *Deep-Sea Research I* 49, 1853–1875.
- Środoń, J., 1981. X-ray identification of randomly interstratified illite/smectite in mixtures with discrete illite. *Clay Minerals* 16, 297–304.
- Środoń, J., Drits, V.A., McCarty, D.K., Hsieh, J.C.C., Eberl, D.D., 2001. Quantitative XRD analysis of clay-rich rocks from random preparations. *Clays and Clay Minerals* 49, 514–528.
- Steineck, P.L., Thomas, E., 1996. The latest Paleocene crisis in the deep sea: Ostracode succession at Maud Rise, Southern Ocean. *Geology* 24, 583–586.
- Thomas, E., 1990. Late Cretaceous through Neogene deep-sea benthic foraminifers (Maud Rise, Weddell Sea, Antarctica). *Proc ODP Sci Results*, vol. 113, pp. 571–594.
- Thomas, E., 1998. The biogeography of the late Paleocene benthic foraminiferal extinction. In: Aubry, M.P., et al. (Ed.), *Late Paleocene–early Eocene biotic and climatic events in the marine and terrestrial records*. Columbia University Press, New York, pp. 214–243.
- Thomas, E., 2003. Extinction and food at the seafloor: a high-resolution benthic foraminiferal record across the Initial Eocene Thermal Maximum, Southern Ocean Site 690. In: Wing, S.L., Gingerich, P.D., Schmitz, B., Thomas, E. (Eds.), *Causes and Consequences of Globally Warm Climates in the Early Paleogene*. Geological Society of America Special Paper, vol. 369. Geological Society of America, Boulder, Colorado, pp. 319–332.
- Thomas, E., McCarren, H.K., 2005. Benthic foraminifera and early Eocene hyperthermal events (SE Atlantic Ocean). Geological Society of America Boulder, CO, United States, vol. 37(7), pp. 413–414.
- Thomas, E., Röhl, U., 2002. The Paleocene-Eocene Thermal Maximum in Ceara Rise Hole 929E. Ocean Drilling Program Leg 154: GSA Annual Meeting, Abstracts, vol. 34, p. 462.
- Thomas, E., Zachos, J.C., 2000. Was the late Paleocene thermal maximum a unique event? *Geologiska Föreningens i Stockholm Förhandlingar (GFF; Transactions of the Geological Society in Stockholm)* 122, 169–170.
- Thomas, E., Zachos, J.C., Bralower, T.J., 2000. Deep-sea environments on a warm Earth: latest Paleocene–early Eocene. In: Huber, B.T., MacLeod, K., Wing, S.L. (Eds.), *Warm Climates in Earth History*. Cambridge University Press, pp. 132–160.
- Tjalsma, R.C., Lohmann, G.P., 1983. Paleocene–Eocene bathyal and abyssal benthic foraminifera from the Atlantic Ocean. *Micropaleontology, Special Publication*, vol. 4, pp. 1–90.
- Tunis, G., Uchman, A., 1998. Ichnology of Eocene flysch deposits in the Carnian pre-Alps (north-eastern Italy). *Gortania* 20, 41–58.
- Tunis, G., Uchman, A., 2003. Trace fossils from the Brkini Flysch (Eocene) south-western Slovenia. *Gortania* 25, 31–45.
- Uchman, A., 2001. Eocene flysch trace fossils from the Hecho Group of the Pyrenees, northern Spain. *Beringeria* 28, 3–41.
- Uchman, A., 2006. Deep-sea ichnology: development of major concepts. In: Miller III, W. (Ed.), *Trace Fossils. Concepts, Problems, Prospects*. Elsevier, Amsterdam, pp. 242–261.
- Uchman, A., Janbu, N.E., Nemeč, W., 2004. Trace fossils in the Cretaceous–Eocene flysch of the Sinop–Boyabat basin, Central Pontides, Turkey. *Annales Societatis Geologorum Poloniae* 74, 197–235.
- Van Morkhoven, F.P.C.M., Berggren, W.A., Edwards, A.S., 1986. Cenozoic cosmopolitan deep-water benthic foraminifera. *Bull. Cent. Rech. Explor.-Product. Elf-Aquitaine, Mem.*, vol. 11.
- Zachos, J., Pagani, M., Sloan, L., Thomas, E., Billups, K., 2001. Trends, rhythms, and aberrations in global climate 65 Ma to present. *Science* 292, 686–693.